COMSOL
CONFERENCE
2024 FLORENCE

Electromechanical Simulations Of High Voltage Equipment

D. Pellegrini[1], G. Tebaldini[1], M. Bonomi[1]
1. Tech department, EB Rebosio – Gruppo Bonomi, Madone (BG), Italy.

Abstract
A substantial campaign of simulations was recently launched in the Bonomi Group with the goal of improving the understanding of the physics involved in high voltage equipment such as aerial power lines, insulators, surge protectors and disconnectors. The activity not only resulted in several product improvements, exploring and introducing a number of new designs, but also allowed the investigation of defects and the possibility to detect them. A selection of the results obtained with the AC-DC and structural mechanics modules will be presented.

Keywords: High voltage, electric field, structural mechanics, insulators, surge arrester

Introduction
Several aspects must be considered to reach a successful designing of a high voltage component such as an insulator or a surge arrester.
Many of the electrical concerns relates to achieving an adequately soft grading of the electrical potential. This limits the peak electric field to values well below the ionization thresholds of the involved materials, air being usually the stricter one. Depending on the case, the problem can be approximated in the electrostatic regime in the frequency domain (eg. AC insulator) or it may require a steady state and even a transient electrodynamic approach (eg. DC insulator, surge arrester).
In addition to electrical aspects, it is often crucial to evaluate structural and mechanical characteristics of the design under development. Such activities include, among others, the definition of a load envelope for multiple interconnected insulators and the determination of the adequacy of a component at sustaining repeated load cycles.

Geometry handling
The whole Gruppo Bonomi relies on Autodesk® Inventor® for 3D modelling. Importing geometries in COMSOL® is seamlessly done by using the *CAD Import Module* which handles several native formats, including Inventor® IPT and IAM. Most of the time very little post processing is required: generally limited to removing excessively small details either by deleting minor components or by means of the *Remove Details* command. To prevent unexpected result arising from evaluating the field at features with discontinuities of the material properties, offset lines and surfaces are introduced directly in COMSOL® by creating work planes, projecting or cross sectioning elements, applying offsets and, eventually, extruding or revolving.

Available hardware
EB Rebosio recently acquired a workstation empowering an AMD® Threadripper® 7970X CPU (32 cores, 64 threads) coupled with 256 GB of DDR5 ECC RAM in quad channel configuration.

Composite Insulators
A high voltage insulator is an electromechanical component which is designed to connect two parts, such as a tower and a conductor cable, subjected to potential differences that could reach the MV regime, containing the current flow between the two while also providing mechanical support for tensile, compressive and/or cantilever loads.
Since more than 20 years EB Rebosio specialized in the production of the composite type of insulators. As depicted in Fig.1, these insulators are composed by a pultruded glass fiber rod with two metal terminals crimped to its ends and an overmolded silicone housing with several sheds. The housing protects the rod from the environment by increasing the insulator resilience to the action of contaminants such as water, carbon and salts [1] [2].

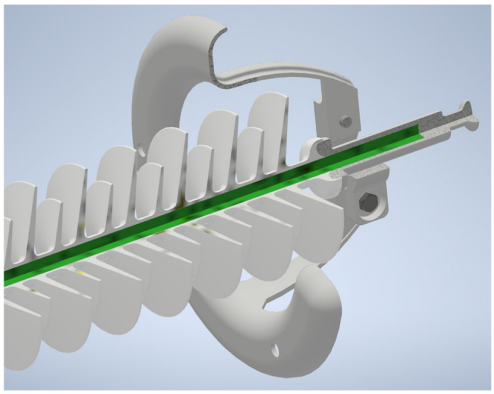

Figure 1. Section view of a composite insulator, including a grading device attached to the end fitting.

A crucial aspect to the lifetime of an insulator is the containment of the value of the electric field on its surface, so that, even in presence of water droplets perturbing the field, the dielectric rigidity of air is never approached. In specific cases this requires the introduction of so-called grading devices (the metal ring surrounding the first sheds in Fig.1), spreading the voltages over larger surfaces and thus limiting the peak electric field.

The accurate evaluation of the applicability of an insulator design to a particular operational scenario requires a complete modelling of the live and ground electrodes, which leads to a 3D computation with the entire insulating chain installed on the tower and a piece of conductor attached to it. The other conductors at the same or different phases should be included as well. The goal of such computation is to provide the field module together with its tangent and normal components close to the insulator surface, usually 0.5 mm from it. Achieving local sub-millimeter resolution in a volume that can be up to 100^3 m^3 is a challenge that only in recent years has become routinely solvable. The aforementioned hardware is definitely capable of handling these problem sizes.

Simulation setup

The simulation setup is significantly different depending on the application: AC or DC. In the AC case the field is governed by capacitive currents with no need to re-evaluate the charge distribution, while in the DC case it is crucial to consider how the charge distribution settles under the influence of resistive currents, no matter how small they can be. Proper modelling of the DC case requires an excellent characterization of the materials, and it is not discussed here. Instead, the AC case requires solving the Gauss Law for the D field (that is the electric field altered by the electric permittivity of the materials), which is handled by the *electrostatic (es)* interface. This also makes the electric permittivity the only relevant material property.

The *Frequency Domain* study allows introducing a sinusoidal time varying magnitude of an otherwise completely static charge distribution as defined by the imposed boundary conditions. The default solver rarely requires any intervention.

The boundary conditions specify ground and live potentials for domains and/or boundaries. If floating metal parts are present, it is important to mark their boundaries with the *Floating Potential* condition, which allows for their electrical potential to be equalized. The outer boundaries of the considered volume can either specify a potential (usually ground), a symmetry condition or an endless boundary condition. For convenience and easiness of the setup, the latter is often replaced with a zero-charge condition, providing that the system boundaries are sufficiently spaced from the areas to be investigated.

Results

The outcome of the setup discussed above is presented in Fig.2. The tower hosts two three-phase circuits, one on each side. The insulator is installed in the middle slot of the left circuit. This kind of global picture allows for a quick evaluation of the correctness of the simulation by checking the electrical potential, especially near the surfaces where it is fixed by the boundary conditions.

Once a global assessment is complete, it is possible to investigate the details of the electric field distribution. The triple point area (the meeting point between the metal terminal, the silicone housing and the air from the environment) is the most critical location of a composite insulator. Not only does its proximity to the terminals naturally subject it to high electric fields which can result in tracking and erosion damage, but it is also the most likely entry point for moisture and pollution. By carefully analyzing the field distribution at the triple point with plots similar the ones presented in Fig.3 and Fig.4, EB Rebosio has been able to review the designs of the silicone-metal junctions harmonizing the requirements from performances and production in a quantitative way.

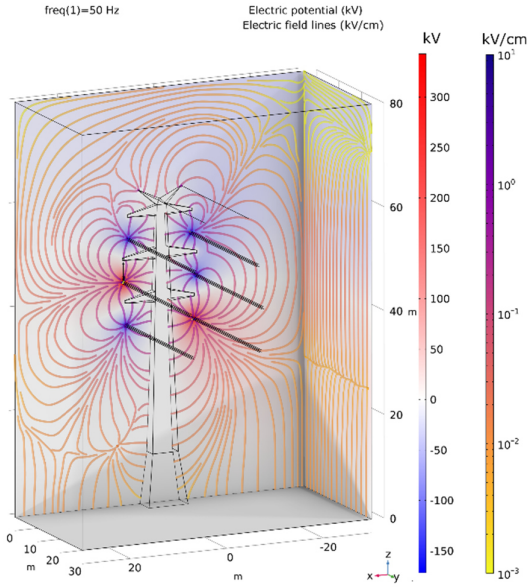

Figure 2. Overview of the electric potential (as surface shading) together with the electric field lines shaded with its magnitude.

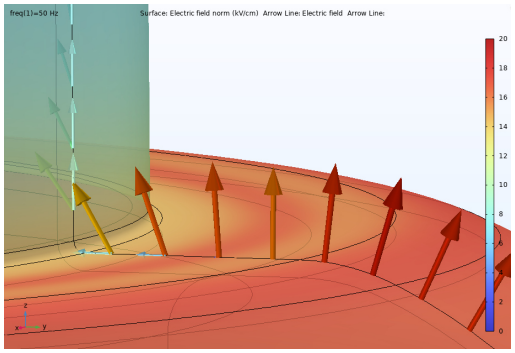

Figure 3. field at the insulator triple point, where silicone, metal, and air meet. The shading representing the field intensity is applied to a surface spaced by 1 mm from the actual insulator surface, thus avoiding material discontinuities. The arrows also visualize both the field module and its component tangent to the surface.

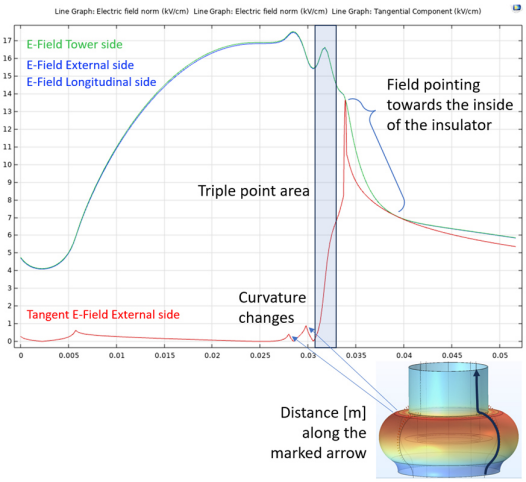

Figure 4. 2D plot of the field magnitude and tangential component collected along a line running in the axial direction and keeping a 1 mm distance from the surface.

For particularly high voltage applications this type of study has been also successfully deployed to investigate the need and the design of additional field mitigating devices such as the grading ring depicted in Fig.1.

Surge arrester

Surge arresters are protective devices that are designed to prevent the spread of voltage spikes to sensitive and expensive devices (such as transformers) by absorbing large amounts of current through them. They do so by employing properly doped pads of ZnO achieving a peculiar voltage-current characteristics that allows them to act almost as insulators during normal operation, while quickly changing to a low impedance path to ground should the voltage surge above the design threshold [3].
Although externally similar to insulators, from the simulation point of view, they are profoundly different as the leakage current through the ZnO core helps further spreading the electrical potential. The study is further complicated by the highly non-linear conductivity which is a function of the electric field permeating the ZnO. This introduces an additional coupling in the equations.
The specific arrester considered here is a multistage arrester, constructed by assembling several modules in a tower. For stability reasons, each tower floor consists of an aluminum base with four arresters in parallel. In total the tower is composed of ten floors.

Simulation setup

The simulation of a surge arrester differs from that of an insulator mainly due to the need to switch to the *electric current (ec)* interface, which, in addition to the Gauss law, allows for charge redistributions in space, deviating from the initial conditions.
The most delicate part of the setup consists in tuning the field-dependent conductivity of the ZnO. The voltage-current characteristics of the ZnO pads is normally available from laboratory measurements.

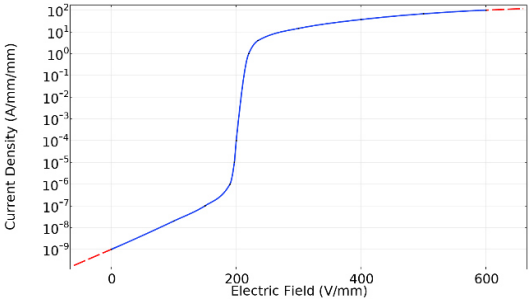

Figure 5. Sample of EJ characteristic for ZnO doped for surge arrester applications.

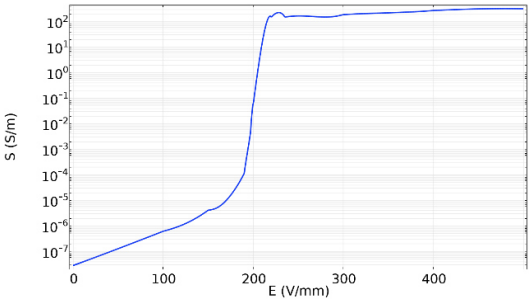

Figure 6. Field dependent conductivity as extracted from the voltage current characteristic measured on a sample.

The first step is to abstract the physical dimensions away by changing the voltage and current to the respective densities, the voltage density being better known as electric field. This results in the EJ material characteristics as exemplified in Fig.5.
Next, the current density axis must be replaced with the conductivity as per COMSOL® input requirements. We start from the Ohm law and from the definition of resistivity ρ:

$$\frac{\mathrm{d}V}{\mathrm{d}I} = R = \rho \frac{L}{A}$$

From there we can write the conductivity S as:

$$S = \frac{1}{\rho} = \frac{1}{R}\frac{L}{A} = \frac{\mathrm{d}I}{\mathrm{d}V}\frac{L}{A} = \frac{\mathrm{d}I/A}{\mathrm{d}V/L} = \frac{\mathrm{d}J}{\mathrm{d}E}$$

If we defined the EJ characteristics as a COMSOL® interpolating function, we just declare an analytical function using COMSOL® differentiating operator:

$$S(E) = \mathrm{d}(EJ(E), E)$$

resulting in the plot shown in Fig.6.
At this point the material conductivity is assigned as the expression:

S(root.comp1.ec.normE)

here S indicates the name of the analytical function.

Convergence could not be obtained by adopting a *frequency domain* study, therefore we setup a *time transient* providing a sinusoidal voltage excitation to the system. Good computational efficiency was obtained by using a fully coupled approach using the PARDISO solver. The non-linear method was switched to the *automatic highly non linear* preset. Sometimes the formation of instable current loops was observed in the highly conductive domains, this was corrected by artificially reducing the aluminum

conductivity, while remaining few orders of magnitude above the one of the ZnO.
Once the transient study was completed, it was possible to switch to the more agile frequency domain study by fixing the conductivity of the ZnO according to the expected field values for the given voltage.
Crucial to the success of this study, was a mesh of exceptionally high quality which was obtained by aggressively removing superfluous details from the geometry and manually meshing most of the domains with a combination of the *edge*, *mapping* and *sweep* commands. The *free tetrahedral* command was only used to fill the irregular domains after all the meshes of the adjacent domains were finalized.

Results

The global picture is inspected for correctness by checking the electric potential distribution, but also the current density distribution and its regularity, as shown in Fig. 7.
The current along the tower has been obtained by integrating the current density over a module cross section. As shown in Fig. 8, below the threshold voltage the current is mostly sinusoidal and carries a capacitive contribution as can be noted by the phase difference with respect to the voltage. As soon as the threshold voltage is exceeded, the current increases rapidly in spikes that are in phase with the applied voltage. This precisely reproduces the behavior observed in lab testing.

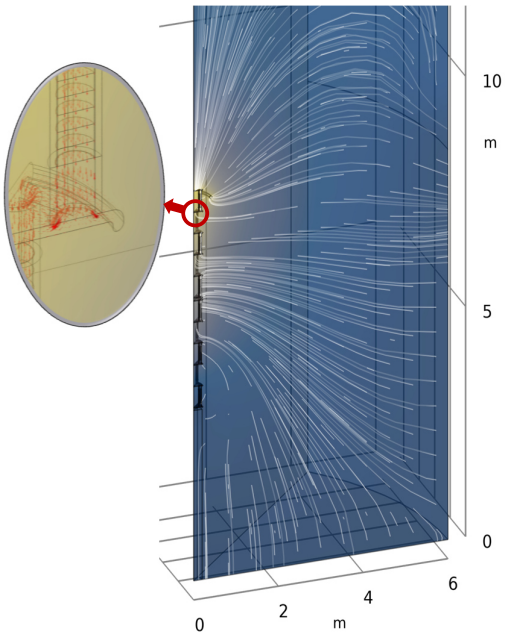

Figure 7. Voltage shading, field lines and current density (as the arrow field in detail) of a 450 kV, 10 stage arrester. The simulation was done profiting from the 8-fold symmetry.

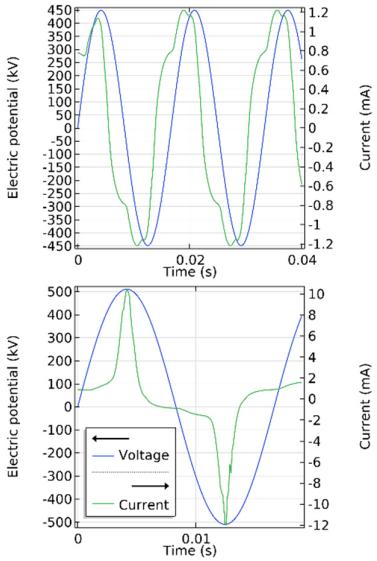

Figure 8. Voltage (input) and current (output) waveforms below (top) and slightly above (bottom) the rapid change of conductivity of the ZnO pads.

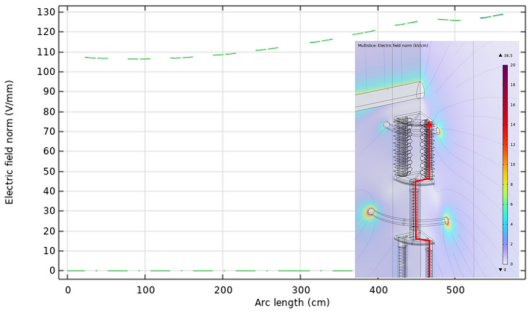

Figure 9. Magnitude of the electric field collected along a path going from the bottom to the top of the tower traversing the ZnO pads.

The evaluation of the electric field at the surfaces proceeds exactly as for insulators. In addition, arresters also require the evaluation of the electric field distribution across the various ZnO pads, so that grading devices could be introduced to balance it reducing their aging impact.

Insulated crossarms

Insulated crossarms are realized by means of two or more insulators, arranged in triangular or pyramidal shapes, so that, in addition to sustaining the conductor, horizontal separation from the pole is provided. Insulated crossarms realized with lightweight composite insulators are gaining traction in aerial powerlines as they allow for more compact and cheaper towers and are suited for line retrofitting.
The basic calculation to provide when designing such a system consists in the load envelope resulting from the allowable loads on each of the selected insulators.

Although the elongation of the insulators could be considered a higher order effect, more complex cases such as a square-base pyramid are hardly solved without considering those.
In these cases, the beam interface in the structural mechanics module comes to the rescue. To facilitate and automate the computation we experimented driving COMSOL® through its powerful Java API. For convenience, the API was accessed in python by leveraging on the MPh opensource project [4] which, in turn, relies on JPype to provide the transition layer to and from Java.

Simulation setup

A very simple COMSOL® template file was setup, defining parameters linked to the geometry and the load to be applied. The mesh only consists of edges with a few intermediate points and the solver was switched to a dense matrix due to the extremely limited number of degrees of freedom.
The Python side consists in a script that loads the COMSOL® template from the disks and proceeds to set it up to communicate the results:

```
client = mph.start(cores=1)
model = client.load(filename.mph)
model.java.result().numerical().create('ep', 'EP')
model.java.result().numerical('ep') \
  .set('expr', 'beam.Nxl')
model.java.result().numerical('ep') \
  .selection().set([1,2,3,4])
```

The last two lines set the beam axial load as output and select all four beams to retrieve the values.
Adjusting the parameters is as simple as:

```
model.parameter(par_name, new_value)
```

The model is solved, and results are retrieved by:

```
model.solve()
result = model.java.result().numerical('ep') \
  .computeResult()
```

This will return a wrapped Java array containing the load decomposed along the axial direction of each insulator.

Results

A simple check consists in ensuring that the load on the crossarm decomposes to values within the specifications of each insulator, such as shown in Fig. 10. However, the real strength of this procedure is the determination of the load envelope by searching, for each polar direction, the maximum load compatible with all the insulators. This is straightforward in Python using the root finding algorithms available from SciPy. The outcome of such computation for the considered crossarm is presented in Fig. 11. For presentation purposes the surface can be cut along the red lines, presenting a set of curves for the horizontal and vertical loads, one for each applied longitudinal load.

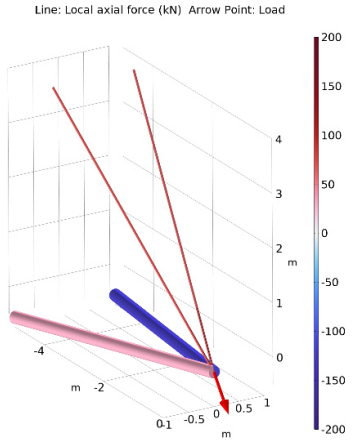

Figure 10. Simple crossarm model setup, showing the reaction of the four insulators to a particular load applied to the tip.

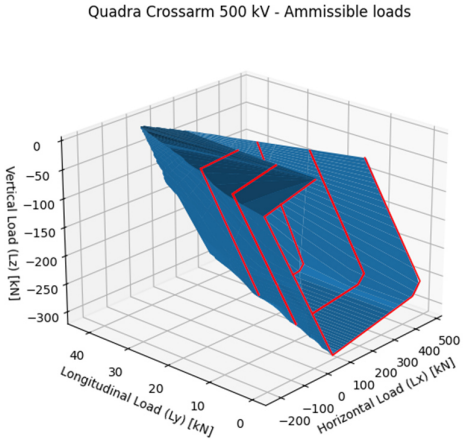

Figure 11. A load envelope computed by searching the maximum admissible load for many polar directions.

Mechanical components

In addition to the “specified load” (which must not result in rupture) components of high voltage lines are usually required to sustain a “maximum design load”, allowing for a perfect return to the initial conditions after its removal.
Given the need of containing weight (and cost) of such parts, FEM analyses play an adamant role in the design process, which would hardly reach proper tuning otherwise.
Typical components which require this kind of analysis are the metal terminals of the so called “post insulators” which employ a large diameter rod to reach large compression and cantilever specified loads.

Simulation setup

This kind of simulation considers various contacts such as between the rod and the terminal and between the terminal and the fixing plate. When

deemed appropriate, the fixing screws are also introduced together with their preload.
With the goal of introducing a load cycle it could be tempting to use a time dependent study, however we found it more convenient to perform a parameter sweep within a stationary study, mostly because this will drop any inertial effect. To succeed in this approach, we start by defining a generic parameter "step" and an interpolated function that specifies the loads for different steps. The function applied to the step is used as the expression for the load boundary condition. This allows to sweep over a monotonic range of steps, while the actual load follows a cycle which generally ramps up and down a couple of times between zero and the load which should allow for a perfect return to zero, before taking it to the specified tensile/compressive/cantilever load which could introduce plasticity but should not exceed the ultimate material stress.
While the material model is continuously improved, for the time being satisfactory results have been achieved considering a bilinear stress curve, which is realized enabling plasticity for a linear elastic material. Future improvements will focus on the proper treatment of the composite rod anisotropy, considering the possibility of the glass fibers to slide with respect to each other in the epoxy matrix.

Results

Figure 12 shows a typical result of this analysis. Here the Von Mises stress is shaded on top of the physical displacement for a cantilever load applied to the tip of the glass fiber rod. On the top left corner, we can see a detail of the hysteresis curve where it can be noted that multiple load cycles come back to zero displacement, while a residual tip displacement of about 2 mm remains after the ramp to the max allowable load.

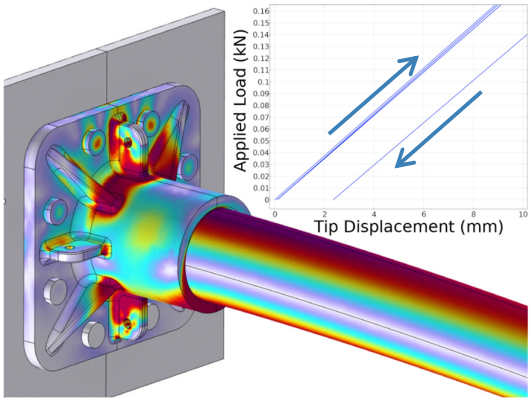

Figure 12. Von Mises stresses at the maximum cantilever load. The box shows the load/displacement hysteresis curve.

Conclusions

The acquisition and large-scale deployment of COMSOL® in EB Rebosio resulted in a significant improvement of the product development cycle. Several uncertainties related to the optimization of the physics involved in the product have been almost cancelled and it is now possible to produce accurate answers in a timely manner on many topics. This not only allowed us to improve the reliability/cost ratio of the products, but also elevated the company image and reputation with the clients.

References

[1] K. O. Papailiou and F. Schmuck, Silicone Composite Insulators Materials, Design, Applications, Springer, 2019.

[2] T. Shaw, EPRI Insulator Reference Book - The Violet Book, Palo Alto, CA: EPRI, 2021.

[3] V. Hinrichsen, Metal-Oxide Surge Arresters in High Voltage Power Systems, Siemens, 2011.

[4] J. Hennig, M. Elfner, A. Maeder and J. Feder, 2024. [Online]. Available: https://doi.org/10.5281/zenodo.11539226.

Acknowledgements

The authors would like to thank Jorge Franco, Giovanni Giobbe and Alberto Scarpetta for their availability in many discussions. They are also grateful to all the clients of EB Rebosio for the stimuli provided.